BOREAL ENVIRONMENT RESEARCH 14: 458–480
ISSN 1239-6095 (print) ISSN 1797-2469 (online)

Helsinki 31 August 2009

Measurements of humidified particle number size distributions in a Finnish boreal forest: derivation of hygroscopic particle growth factors

Wolfram Birmili[1)], Kathrin Schwirn[1)], Andreas Nowak[1)], Tuukka Petäjä[2)], Jorma Joutsensaari[3)], Diana Rose[1)], Alfred Wiedensohler[1)], Kaarle Hämeri[2)], Pasi Aalto[2)], Markku Kulmala[2)] and Michael Boy[2)]

[1)] *Leibniz Institute for Tropospheric Research, Permoserstrasse 15, D-04318 Leipzig, Germany*
[2)] *Department of Physics, P.O. Box 64, FI-00014 University of Helsinki, Finland*
[3)] *University of Kuopio, Department of Physics, P.O. Box 1627, FI-70211 Kuopio, Finland*

Received 19 May 2008, accepted 21 Oct. 2008 (Editor in charge of this article: Veli-Matti Kerminen)

Birmili, W., Schwirn, K., Nowak, A., Petäjä, T., Joutsensaari, J., Rose, D., Wiedensohler, A., Hämeri, K., Aalto, P., Kulmala, M. & Boy, M. 2009: Measurements of humidified particle number size distributions in a Finnish boreal forest: derivation of hygroscopic particle growth factors. *Boreal Env. Res.* 14: 458–480.

Dry and humidified size distributions of atmospheric particles were characterised at the atmospheric research station SMEAR II, Finland between May and July 2004. Particles were classified in a size range between 3 and 800 nm at controlled relative humidities up to 90% by two instruments complementary in size range (HDMPS; Nano-HDMPS). Using the summation method, descriptive hygroscopic growth factors (DHGF) were derived for particle diameters between 70 and 300 nm by comparing dry and humidified size distributions. At 90% relative humidity, DHGF showed mean values between 1.25 and 1.45 in the accumulation mode, between 1.20 and 1.25 in the Aitken mode, and between 1.15 and 1.20 in the nucleation mode. Due to the high size resolution of the method, the transition in DHGF between the Aitken and accumulation modes, which reflects differences in the soluble fraction, could be pinpointed efficiently. For the accumulation mode, experimental DHGFs were compared to those calculated from a simplistic growth model initialised by *in-situ* chemical composition measurements, and yielded maximum deviations around 0.1. The variation in DHGF could only imperfectly be linked to meteorological factors. A pragmatic parameterisation of DHGF as a function of particle diameter and relative humiditity was derived, and subsequently used to study the sensitivity of the condensational sink parameter (CS) as a function of height in a well-mixed boundary layer.

Introduction

Atmospheric aerosol particles are known to absorb water vapour at relative humidities well below supersaturation (Orr *et al*. 1958). Consequently, the ambient diameter of a particle will depend on the relative humidity (RH) given at a specific time. This hygroscopic growth has immediate consequences on atmospheric visibility (Tang *et al*. 1981) and the scattering of downwelling and upwelling solar radiation (Ogren and Charlson 1992). The hygroscopicity

of particles is also connected with their ability to act as a cloud condensation nucleus (Eichel *et al*. 1996, Khvorostyanov and Curry 1999). A further implication is that the progression rates of aerosol dynamic processes in the atmosphere, involving coagulation, condensation, and deposition will also depend on ambient RH. A review of global aerosol transport models has identified hygroscopic particle growth as a significant source of uncertainty when predicting radiative forcing (Kinne *et al*. 2003).

The degree of water absorption depends, in general, on the number of soluble molecules and ions per volume of dry particle material (e.g. Hänel 1976, Thudium 1978). While the hygroscopic growth of pure soluble ionic species is known relatively accurately (Tang and Munkelwitz 1994, Brechtel and Kreidenweis 2000), the growth of atmospheric organic matter (Saxena and Hildemann 1996, Gysel *et al*. 2004) or complex mixtures of various substances that are typical for the atmosphere is more uncertain. In an attempt to provide a simple but workable description of atmospheric aerosols, empirical expressions have been derived for the hygroscopic growth as a function of relative humidity (Hänel 1976).

Earlier experimental methods used gravimetry (Winkler 1972, Hänel and Lehmann 1981) or the change of the integral light scattering signal (Gassó *et al*. 2000, Im *et al*. 2001) to quantify the water uptake of atmospheric aerosols. The tandem differential mobility analyser (HTDMA, Rader and McMurry 1986) has been designed to measure the hygroscopicity of a monodisperse selection of aerosol particles. A major asset of the HTDMA technique is that it resolves external particle mixtures. Recent developments of the HTDMA have aimed at extending the measurement range into the nucleation mode (Väkevä *et al*. 2002) as well as RHs above 90% (Weingartner *et al*. 2002, Hennig *et al*. 2005). With the HTDMA, a considerable body of sub-μm hygroscopic particle growth factor data has been collected in many atmospheric environments (*see* Swietlicki *et al*. 2008, and references therein). The population of atmospheric sub-μm particles is an external mixture of more and less hygroscopic particles, while their hygroscopic growth intensifies when passing from the nucleation mode to the accumulation mode (Swietlicki *et al*. 2008). Laboratory and field experiments have also characterised aerosols near source, such as diesel exhaust (Weingartner *et al*. 1997) or biomass burning aerosols (Rissler *et al*. 2006).

A relatively new method to infer particle hygroscopic growth is based on the concurrent measurement of complete dry and humidified particle size distributions by electro-mobility analysers (Birmili *et al*. 2004). This work's intention was to explore this technique in the atmosphere over the boreal forest and provide representative humidified number size distributions. Hygroscopic particle parameters in a continental background environment are of interest with respect to the properties of freshly formed nucleation mode particles as well as the role of pre-existing particles on particle nucleation under ambient conditions. Hygroscopic particle growth factors are examined as a function of particle size, chemical composition as well as meteorological parameters. The work concludes with a sensitivity study of the potential role of hygroscopic particle growth on the condensation sink (CS), which is an essential dynamic parameter for the modelling of gas phase constituents and new particle formation.

Methods

Field experiment

The FIGARO field experiment (Finnish–German Atmospheric Research Co-operation) was conducted between May and July 2004 at the atmospheric research station SMEAR II in Hyytiälä (61°51´N, 24°17´E, 181 m a.s.l.), approximately 220 km north of Helsinki, Finland. SMEAR II is an extensively equipped research station for measuring ecosystem–atmosphere relations (Hari and Kulmala 2005), and is surrounded by a homogeneous Scots pine stand. Measurements took place between 6 May and 7 July 2004, a period subsequently denoted as days of year (DOY) 127–191. Aerosol measurements were conducted from inside a temperature-controlled container laboratory. Due to lack of space near the SMEAR II main station, the container was positioned on a forest path approximately 50 m

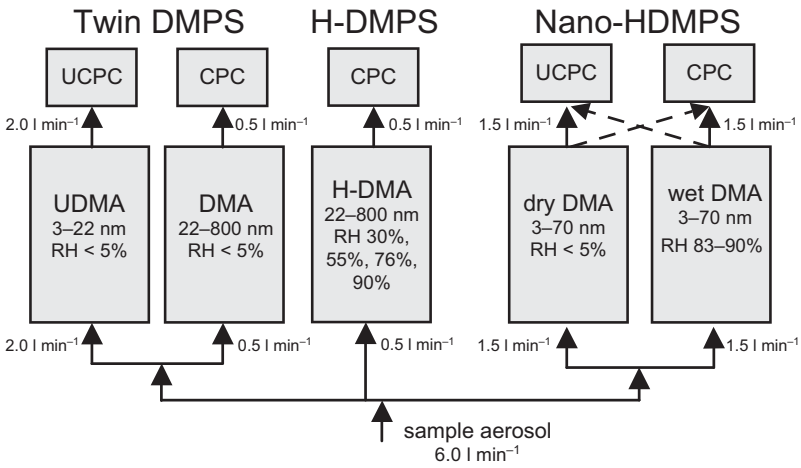

Fig. 1. Parallel size distribution measurements using a twin DMPS, a humidifying DMPS (HDMPS) and a Nano-HDMPS. During FIGARO, the HDMPS was operated in subsequent cycles of 30%, 55%, 76% and 90% relative humidity, while the Nano-HDMPS (wet) stayed between 80% and 90%.

south of the station. Ambient air was sampled from an Andersen PM_{10} inlet at a height of 6 m above the ground, with the height of the surrounding trees being between 10 and 20 m. The size distribution measurements in the container laboratory involved parallel operation of a twin differential mobility particle sizer (TDMPS), a humidifying differential mobility particle sizer (HDMPS), and a dry and wet Nano-HDMPS, respectively (Fig. 1).

TDMPS instrument

Dry particle size distributions were measured every 10 minutes across a particle size range of 3–900 nm using a twin differential mobility particle sizer (TDMPS; Birmili *et al*. 1999). This instrument has been used for short-term measurements as well as long-term monitoring (Birmili *et al*. 2003, Engler *et al*. 2007). Briefly, the TDMPS consists of two Vienna-type differential mobility analysers (Vienna DMA; Winklmayr *et al*. 1991) having centre rod lengths of 11 and 28 cm, respectively. The sheath-to-aerosol flow ratio in the short DMA was 20:2.0 l min^{-1}, and 5.0:0.5 l min^{-1} in the long DMA. Condensation particle counters (UCPC 3025 A and CPC 3010; TSI Inc., St Paul, U.S.A.) counted monodisperse particles downstream of each DMA. The DMA aerosol inlet flows were controlled to within 1% by automatic flow regulation while the sheath air was prepared using a regenerative diffusion dryer. When entering the instrument, the relative humidity of the sheath air was below 5%, i.e. the instrument yields dry reference size distributions. Raw mobility distributions were inverted using a multiple charge inversion taking CPC collection efficiencies and DMA transfer functions into account. The absolute measurement uncertainty of the TDMPS with respect to total particle number concentration is assumed to be 10%.

HDMPS instrument

Humidified particle size distributions were measured over a particle size range of 22–900 nm using a novel instrument, the humidifying differential mobility particle sizer (HDMPS) (Nowak 2006). The principle of the HDMPS system (Fig. 2) closely follows that of the DMPS except that particle size distributions are recorded at controlled RH.

In the instrument, sample aerosol was firstly humidified to approximately 90% relative humidity in a Nafion™ pre-humidifier (MH-110-12-S, ANSYCO Inc., Karlsruhe, Germany). Pre-humidification ensured that the sample aerosol particles originated from a state above the deliquescence points of inorganic soluble species that are relevant in atmospheric aerosols. During the campaign the relative humidity in the pre-humidifier was within 85.4%–93.4%, being on average 88.8% (± 1.0%). Secondly, aerosol was conditioned to the target RH by a membrane diffusion dryer (MD-110-12-F, ANSYCO Inc.).

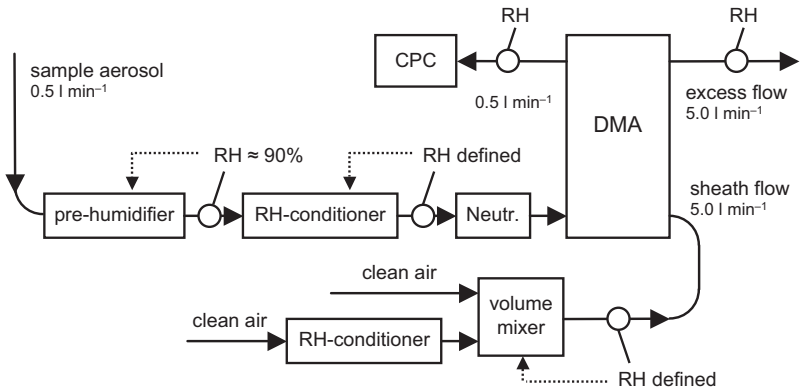

Fig. 2. Principle of the humidifying differential mobility particle sizer (HDMPS). Dotted lines indicate feedback regulation. CPC: Condensation particle counter; DMA: Differential mobility analyser; Neutr.: Charge neutraliser.

Importantly, the aerosol was brought to the selected target RH before passing through the bipolar charger. This ensured that the bipolar charge equilibrium was achieved under the same relative humidity as during the subsequent classification in the DMA. Any deviation from this procedure might render the assumptions on the bipolar charge equilibrium invalid.

Using a second humidifier, the DMA sheath air was continuously prepared at the target RH (Fig. 2). The HDMPS can measure particle number size distributions at any fixed RH between 20% and 90%. The lower limit of this range is given by the capacity of the membrane diffusion dryer to desiccate the pre-humidified aerosol. Its upper limit is defined by the instrument's ability to stably maintain such high RH. The relative humidities, temperatures, and flows inside the HTDMA were continuously monitored using temperature/humidity sensors (HMP230, Vaisala Inc., Helsinki, Finland) and differential pressure transducers (*see* Fig. 2). All humidity sensors were calibrated prior to and after the experiment using a dew point mirror (DewPrime II Dew Point Hygrometer, Model 2002, Edge Tech, Marlborough (MA), USA), which is more accurate than the HMP230. At 90% RH, the manufacturers give absolute uncertainties of 1% (HMP 230), and 0.5% (DewPrime II), respectively, so that an overall of ±1% accuracy of the 90% RH measurement could be ensured. When considering error propagation this uncertainty in RH translates into an accuracy of ±0.02 in the hygroscopic particle growth factors derived later.

Our practice during FIGARO was to record humidified particle size distributions in successive measurement cycles, so that a picture of particle hygroscopicity over a range of RH as wide as possible was obtained (Fig. 3). During successive measurements at the discrete RH-levels of 30%, 55%, 76% and 90%. Each cycle consisted of three size distribution scans except at 90% RH, where five size distributions were measured due to the lower stability of the humidity regulation. The times required for a measurement cycle were 30 minutes at each RH except 50 minutes at 90% RH. Adding time for the stabilisation of RH prior to each cycle, the complete characterisation of an aerosol at all four RHs required three hours.

The combined TDMPS and HDMPS measurements between 6 May and 7 July 2004 were quality controlled using the logged instrumental humidities, temperatures, and air flows (*see* Table 1 for ranges of humidities and temperatures requested for valid measurements, as well as their average values during the campaign). The sheath air RH was the most stable because it was regulated towards a set point. All other parameters were non-regulated and, thus, of higher variance. During quality control, the data were screened particularly for extreme deviations in RH between the excess and the sheath air, which might be indicative of temperature instabilities inside the instrument and/or the laboratory container. A maximum deviation of 1.2% RH was accepted, which is an arbitrary value but likely reflects the limitations of the instrumentation. As a result of the quality control, approximately 25% of the HDMPS data had to be excluded from further analysis leaving a total of 3768 individual measurements at four RHs.

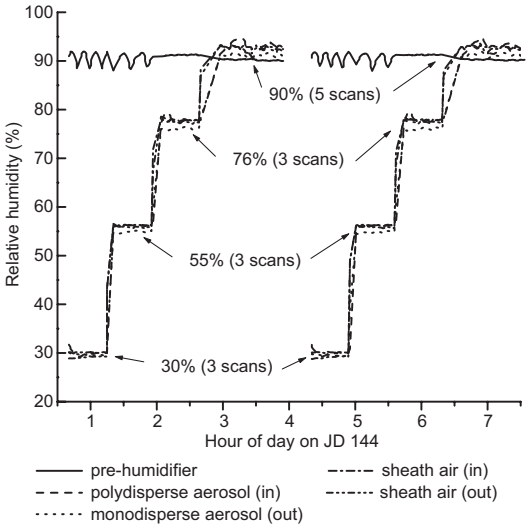

Fig. 3. Exemplary time series of RH measured in different sections of the HDMPS instrument.

The evaluation of the HDMPS data involved, in addition to the procedure described for the TDMPS, an instrumental correction for the diffusional particle losses inside the Nafion™ aerosol pre-humidifiers and aerosol dryers. To account for these losses, a lump correction factor function was developed by comparing particle number size distributions of the TDMPS and the HDMPS collected under similar conditions. For the best comparison, the ambient measurements of the HDMPS at 30% RH during FIGARO were employed, which corresponds to about 20% of all size distributions collected during the campaign (Fig. 4). At 30% RH, the hygroscopic growth of the particles is still modest and only marginally distorts the size distribution. Still, the particle diameters of the HDMPS distributions were adjusted by a factor of 0.95 to match the slope of the TDMPS distribution in the range > 100 nm, thereby accounting for the hygroscopic growth occurring between 5 and 30% RH. The two instruments agree well (within 3%) in their readings across the upper part of the size distribution (*see* Fig. 4). Below 100 nm, a reduced particle transmission through the HDMPS was identified as follows: 0.95 (75 nm), 0.92 (42 nm), 0.86 (35 nm) and 0.54 (25 nm). From the data presented in Fig. 4, an efficiency curve was derived, which was subsequently applied as a final correction to the HDMPS number size distributions.

It was our observation that even after correcting the HDMPS data, the total number concentrations under the HDMPS occasionally underestimated the corresponding values under the TDMPS distribution, especially at higher RH. Our impression was that the HDMPS particle loss correction, developed for 30% RH, might underestimate the real losses at higher RH. Since we were not able to derive the true correction for all relative humidities, these uncertainties and their implications are discussed below.

Determination of hygroscopic growth factors

While the HTDMA technique provides size-resolved hygroscopic particle growth factors directly, the combined TDMPS/HDMPS technique requires an additional data evaluation step. For the TDMPS/HDMPS technique we have developed a summation method (SM) that extracts hygroscopic particle growth from the dry and humidified particle number size distributions (Birmili *et al*. 2004). Since the SM derives growth factors averaging over all hygro-

Table 1. Instrumental parameters (mean ± 1 SD) in the HDMPS during FIGARO for each relative humidity mode.

RH cycle	RH = 30%	RH = 55%	RH = 76%	RH = 90%
RH (sheath air)	30.00 ± 0.01	55.00 ± 0.01	75.99 ± 0.03	90.00 ± 0.02
maximum range	29.9 to 30.0	55.0 to 55.0	75.9 to 76.1	89.9 to 90.2
RH (excess air)	29.34 ± 0.31	55.03 ± 0.25	76.1 ± 0.36	90.25 ± 0.43
maximum range	28.4 to 31.6	54.4 to 55.5	75.2 to 77.0	89.1 to 91.2
ΔRH (excess-sheath air)	–0.66 ± 0.31	–0.02 ± 0.25	0.11 ± 0.36	0.25 ± 0.43
maximum range	–1.64 to 1.62	–0.59 to 0.49	0.85 to 1.04	–0.89 to 1.20
ΔT (excess-sheath air)	–0.04 ± 0.13	–0.04 ± 0.6	–0.04 ± 0.8	–0.04 ± 0.8
maximum range		–0.19 to 0.11	–0.21 to 0.15	–0.23 to 0.15

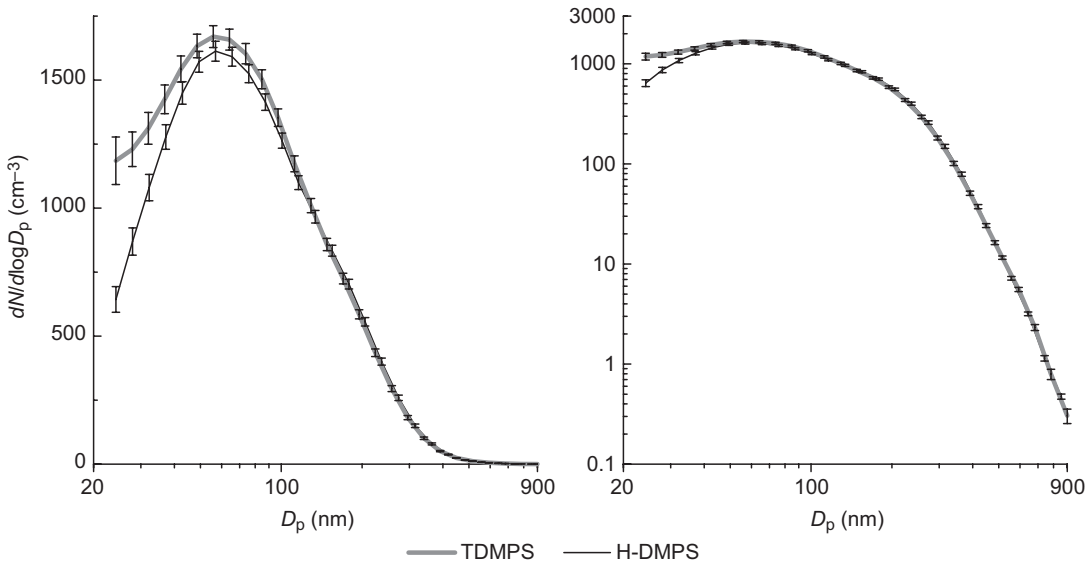

Fig. 4. Comparison of the HDMPS (30% RH) and TDMPS (RH < 5%) average number size distributions during FIGARO before correcting the HDMPS data. The particle diameters of the HDMPS distributions were adjusted by a factor of 0.95 to match the TDMPS data in the range > 100 nm. The calculations account for the multiple charge correction, the DMA transfer function, and the CPC counting efficiencies.

scopic particle fractions, its output function was termed Descriptive Hygroscopic Growth Factor (DHGF).

The SM requires the basic assumption that the total number under the particle size distribution remains constant during the humidification process. This conservation of particle number requires that particles are neither produced nor lost during the experimental process. Statistically speaking, a particle appearing in the TDMPS will be detectable in the HDMPS, however, at a different diameter. The process of humidification of the dry particle distribution in the HDMPS can thus be considered a size distribution rearrangement. In the following we assume that these requirements are met, with limitations of the assumption and their implications being addressed later.

In the first step, the SM splits the dry size particle distribution into a number of disjunctive size distribution segments (slices) that have equal number concentration. In practice, 500 segments are used per distribution, which leads to a typical size of a single segment between 1 and 10 particles per cm^3. It is worth mentioning that the many segments usually have different widths in terms of diameter, depending on the particular shape of the size distribution. The SM now allocates two corresponding size distribution segments (slices), one under the dry and one under the humidified size distributions to each other. The allocation procedure starts with the uppermost segment in each size distribution. This can be understood in a statistical sense that the biggest particles under the dry distribution convert into the biggest particles under the wet distribution. This appears a reasonable assumption as long as no extreme stepwise changes occur in particle hygroscopicity along with diameter.

Once two corresponding size distribution segments have been allocated, the descriptive hygroscopic growth factor is computed by dividing the mean particle diameters of the "wet" size distribution segment by the diameter of the corresponding "dry" segment: DHGF = $D_{p(wet)}/D_{p(dry)}$. This first data point provides the DHGF at the upper tail of the size distribution. The procedure then continues by allocating the two "wet" and "dry" segments that are the lower-sized neighbours to the two segments evaluated treated above. The two new segments will have different diameters, probably different widths, but encompass in any case the same the same number concentration as their upper neighbours.

DHGF is again calculated as above and the procedure repeated until the lower-sized end of the particle number distributions is reached.

As a result of the SM, a descriptive growth factor curve DHGF ($D_{p(dry)}$) having about 500 data points is obtained for each pair of concurrently measured dry and humidified distributions. Since the bins of the DHGF are usually different as a result of different size distribution shapes, the DHGF curves were re-binned onto a constant grid ranging between 30 and 300 nm.

One might argue that the allocation of particle number segments as executed in the SM is not suitable because atmospheric aerosol populations are usually externally mixed with regard to their hygroscopicity (Swietlicki *et al*. 2008), and that the SM ignores this fact. The DHGF curve obtained by the SM, however, may also be described as the "rule" that converts a wet particle number size distribution into a corresponding dry distribution and vice versa. Numerical tests, not shown here, confirmed that the inverse application of DHGF onto a dry distribution restores indeed the original wet size distribution. As a consequence, the interpretation of DHGF as a mean growth factor of a given dry particle size is valid as long as no extreme stepwise changes occur in particle hygroscopicity as a function of particle diameter. This DHGF integrates, of course, over all sub-populations of less and more hygroscopic particle, and can therefore be compared only to HTDMA data averaged over all hygroscopicity classes.

Measurements with a HTDMA during FIGARO (not shown due to limited data quality) revealed that the hygroscopic mixture of sub-μm aerosols was overwhelmingly monomodal, i.e. 80% and more of the particle population belonged to the more hygroscopic particle mode. This trend even increased from 50 towards 250 nm dry size. This observation suggests that the SM generates a parameter that closely corresponds to a growth factor of real particles.

The accuracy of the derived DHGFs might be influenced by systematic as well as accidental errors. We tested the sensitivity of the derived DHGF towards artificial deviations in the number size distribution data, using the median number size distributions (*see* Fig. 5). When adding a bias of 5% in total particle number to the HDMPS distribution, DHGF (at 90%) increased by 0.05 at 73 nm, and by 0.10 at 30 nm, while the changes remained smaller than 0.02 above 180 nm. Subtracting 5% from the particle number led to a change in DHGF of the opposite sign. The sensitivity was also tested for size-dependent deviations, similar in structure to those determined by the HDMPS/TDMPS comparison at 30% RH. Deviations were artificially introduced, ranging between a collection efficiency of only 60% at 20 nm, and 100% at 100 nm, and interpolating linearly as a function of the logarithm of particle diameter. Here, we found that changes in DHGF were negligible across the size range 70–300 nm. At 30 nm, however, DHGH would decrease by 40%.

As a consequence of these sensitivity tests, we confined our interpretations of DHGF to the dry particle size range 70–300 nm. As can be seen in the Results, this is also the range where the DHGFs show a consistent and monotonous behaviour with particle size. An extension of the size range of 70–300 nm is a goal for the future, but will require more sophisticated calibrations and instrumental comparisons involving the HDMPS.

Nano-HDMPS instrument

In addition to the HDMPS described above, humidified and dry particle size distributions were measured every 10 min across the particle size range 3–70 nm with the Nano-HDMPS instrument. The Nano-HDMPS consists of two subsystems, wet and dry DMPSs (Fig. 1). In the wet DMPS, aerosol particles are humidified to about 90% RH with water vapour before charging and particle size measurement. The system consists of a Gore-Tex™ type aerosol humidifier, a Vienna-type DMA (electrode length 10.9 cm), a sheath air humidifier and a CPC (TSI model 3025, or 3010). The sheath-to-aerosol flow ratio was 10:1.5 l min^{-1}. The construction of the instrument closely follows the hygroscopicity tandem DMA described by Joutsensaari *et al*. (2001). The dry DMPS is similar to the wet DMPS except that particles are measured at RH below 10%. Wet and dry measurements were conducted simultaneously but the CPCs were switched during

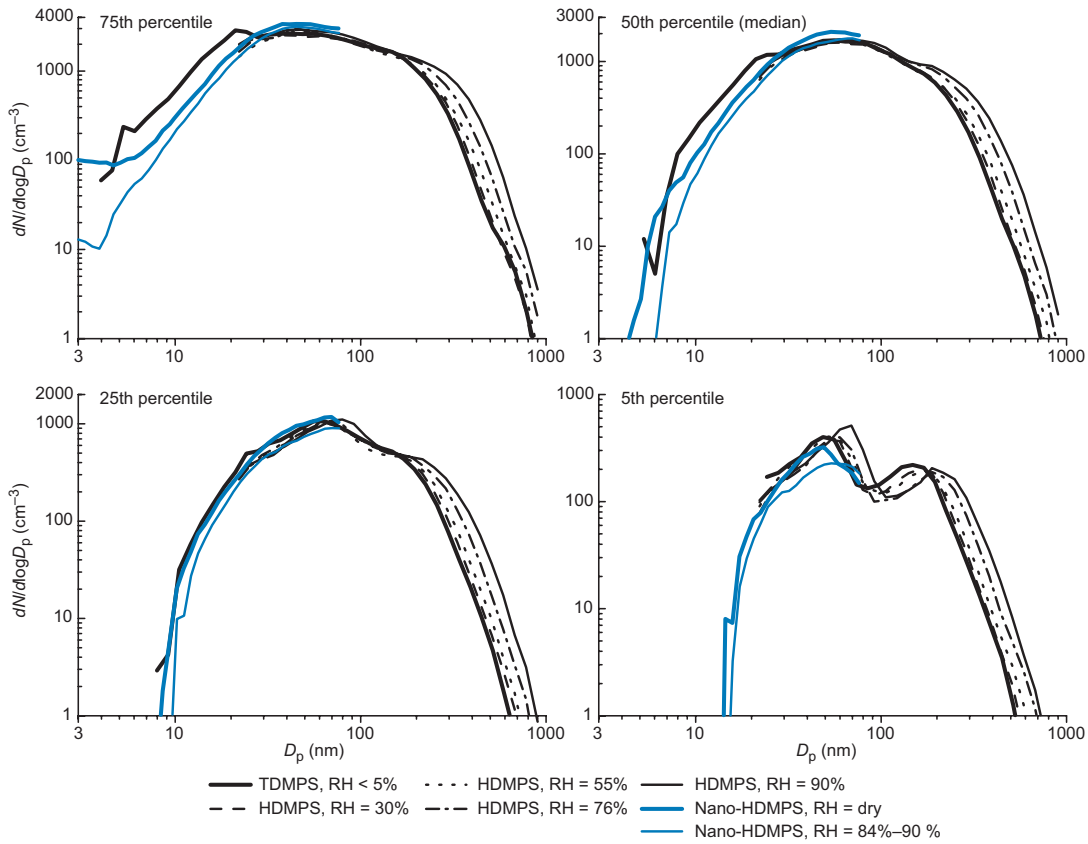

Fig. 5. Different statistical levels of dry and humidified atmospheric number size distributions measured with multiple instruments during FIGARO. The data set includes a total of 3768 size distributions.

consecutive measurements (*see* Fig. 1).

Particle size distributions were determined from raw mobility distributions using a Tichonov regularization method with a smoothness constraint (Voutilainen *et al*. 2001). In the inversion, the particle size range considered was expanded to 70–200 nm to account for the effects of multiply charged particles. CPC counting efficiencies and diffusional particle losses in the tubing and the DMA were included in the evaluation. Furthermore, any difference in absolute particle concentration between the CPC 3025 and CPC 3010 was taken account, always using the CPC 3010 as a reference on the basis of average values over several days. Here, results using the CPC 3025 are presented.

Hygroscopic particle growth factors (GF) were calculated as the ratio of the geometric mean diameters (GMD) of the dry and humidified particle size distributions. In the calculations of GMDs, changes of the upper and lower limits of size ranges due to growth of particles were corrected assuming that GF is 1.12 and 1.22 for 3 nm and 70 nm particles, respectively. The value of 1.12 is consistent with the hygroscopic growth factor of 3 nm ammonium sulphate particles at 90% RH (Hämeri *et al*. 2000), while 1.22 corresponds to an ambient growth factor of 70 nm at 90% RH measured for continental background (Nessler *et al*. 2003). These starting assumptions are necessary when defining the (moveable) integration ranges for the calculation of the geometric mean diameter (GMDs) from the dry and wet Nano-HDMPS. It is worth to note that unlike for the HDMPS, the summation method could not be used because the Nano-HDMPS distributions are not sufficiently wide to encompass a majority of total particle number.

Average GFs were subsequently calculated for different dry particle size ranges (10, 30

and 50 nm, ± 10 nm each). A few individual GF values outside the range 0.8–1.8 were excluded from further data averaging because they lie outside the plausible range defined by collapsing fractal agglomerates on the lower edge (~0.8), and pure ammonium sulfate at the upper edge (~1.8). We suspect malfunctioning equipment as the cause of these values. Also, the dry and wet particle size distributions were not measured exactly simultaneously but consecutively at a 10-minute delay in the Nano-HDMPS due to CPC switching. Rapid changes in the particle size distribution may therefore propagate into the derived GF and generate unrealistic values.

Results

Size distribution

The HDMPS data include the empirically derived size-dependent correction for particle losses in their humidification and desiccation components. To encompass the different degrees of the atmospheric particle concentration at the SMEAR-II station, we present 75th, 50th, 25th and 5th percentiles of the size distributions (Fig. 5). The hygroscopic particle growth can be recognised easily in the accumulation mode on the right-hand side of the distributions (*see* Fig. 5). In the 5th percentile distribution, which is clearly bimodal, a hygroscopic growth of the Aitken mode is also evident (*see* Fig. 5).

Case studies

A general observation is that the humidification preserves the multi-modal shapes of the dry distributions, although larger particles tend to show higher growth factors (Fig. 6). The total particle number concentration did not necessarily correlate with the particle volume: as depicted in Fig. 6c, e, g and i, air masses where a nucleation or Aitken mode indicates the previous formation of new particles. In these four cases the air from the Barents Sea or the North Atlantic passed over the northern areas of Norway and Finland, so that the precursors are likely to originate from the boreal vegetation as described in Tunved *et al*. (2006).

The summation method was used to generate descriptive hygroscopic growth factors (DHGF) as a function of dry particle size for each pair of valid dry and humidified number size distributions. There is a general trend from higher DHGFs (mean values between 1.35 and 1.50 at 90% RH) at particle sizes (200–300 nm) towards lower DHGFs at smaller particle sizes (< 100 nm) (Fig. 6). It is evident that hygroscopicity changes may occur between several tens of nanometers in dry diameter (Fig. 6d). This behaviour can only be explained by an associated change in chemical particle composition because the influence of the Kelvin and Raoult effects is far smaller than the observed differences (*see* Fig. 7). The accumulation mode in Fig. 6d, for instance, shows a DHGF up to ~1.6 whereas the Aitken mode has only a DHGF of ~1.2. In between, at 80 nm a minimum occurs with a growth factor as low as 1.1. It is noteworthy that the size-dependent behaviour of the DHGF is in accordance with the physical structure of the size distribution: The minima of the DHGF and the dry particle number size distribution in Fig. 6d coincide exactly.

The size-selective transition in hygroscopic behaviour

The high size-selective resolution of the derived DHGFs is a significant asset of the TDMPS/HDMPS method, since it allows to pinpoint the diameters relatively accurately, where the chemical transition between the Aitken and accumulation modes occurs (Fig. 7). The hygroscopic growth factors of accumulation mode particles can be seen in the range 1.4–1.7, corresponding to higher fractions of soluble chemical species. In a few cases, the observed particle growth factors correspond to those of pure ammonium sulphate particles. Aitken mode particles, in contrast, are less hygroscopic, at growth factors mostly between 1.15 and 1.45. This trend towards lower growth factors in the Aitken mode coincides with former HTDMA observations at the SMEAR-II station (Hämeri *et al*. 2001, Petäjä *et al*. 2005, Ehn *et al*. 2007) but also other sites (Swietlicki *et al*. 2008).

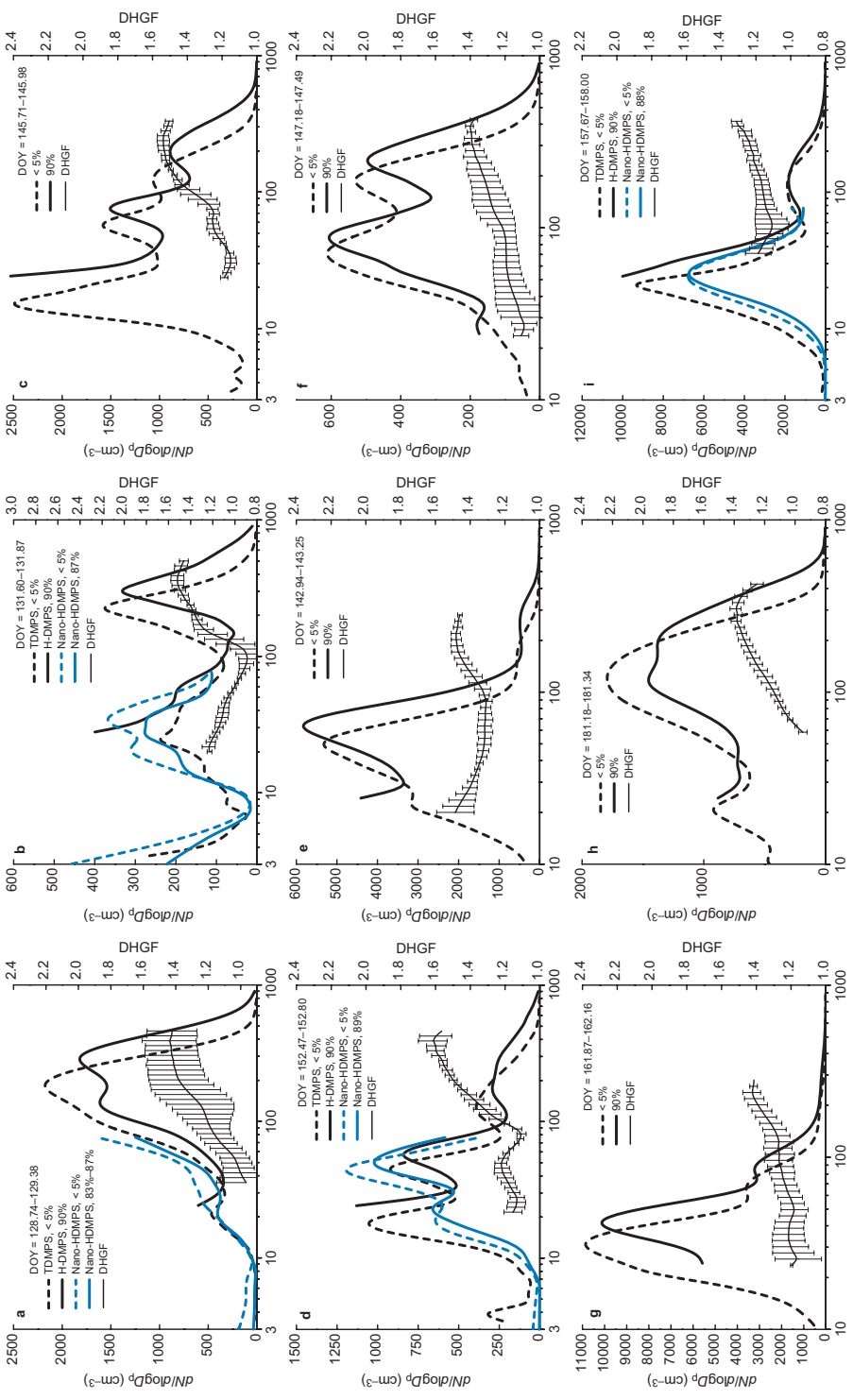

Fig. 6. Average particle number size distributions (dry and humidified [90% RH]), and descriptive hygroscopic growth factors (DHGF) for case studies during FIGARO; DOY = day of year. (**a**) polluted continental air from central Russia (particle number concentration 1580 cm^{-3}; particle volume concentration 6.9 µm^3 cm^{-3}), (**b**) clean Arctic air (330 cm^{-3}; 1.4 µm^3 cm^{-3}), (**c**) slowly moving Arctic air with recent new particle formation (1940 cm^{-3}; 1.2 µm^3 cm^{-3}), (**d**) North Scandinavian air (850 cm^{-3}; 1.1 µm^3 cm^{-3}), (**e**) clean Arctic air from high latitudes with recent new particle formation (3180 cm^{-3}; 1.0 µm^3 cm^{-3}), (**f**) slowly moving Arctic air with anthropogenic influence (530 cm^{-3}; 1.5 µm^3 cm^{-3}), (**g**) North Atlantic air with recent new particle formation (5400 cm^{-3}; 0.9 µm^3 cm^{-3}), (**h**) continental air from northern Russia (1710 cm^{-3}; 3.3 µm^3 cm^{-3}), (**i**) North Atlantic air with recent new particle formation (4700 cm^{-3}; 2.1 µm^3 cm^{-3}).

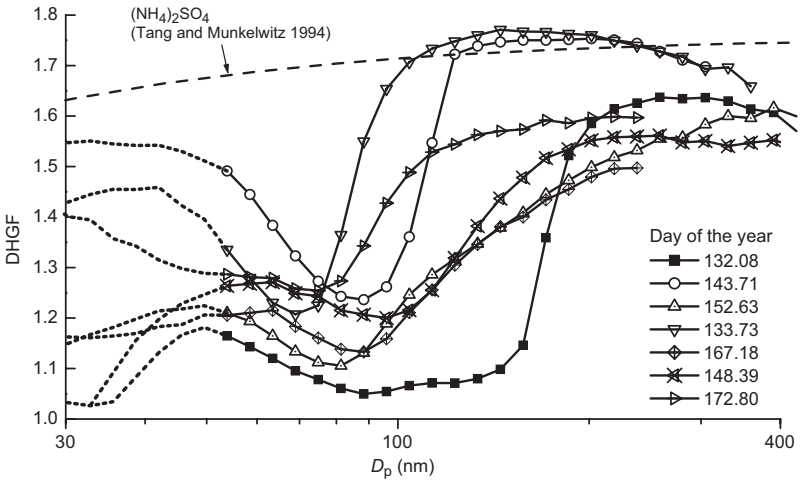

Fig. 7. Descriptive hygroscopic growth factors (DHGF) at 90% RH determined from HDMPS/TDMPS as a function of particle size. Shown are seven case studies when extreme differences in DHGF were encountered between the Aitken and the accumulation mode. Dashed lines mark the area (D_p < 50 nm) where the DHGFs are expected to be of higher uncertainty.

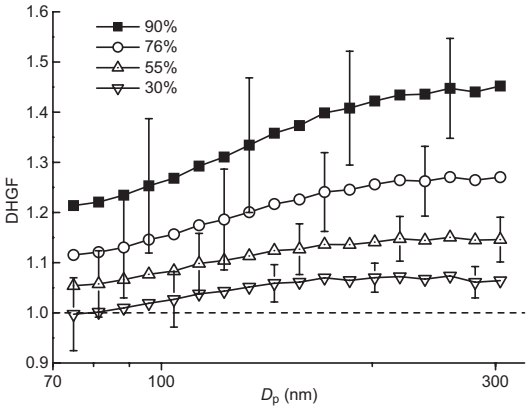

Fig. 8. Grand average of the descriptive hygroscopic growth factor as a function of particle size for all RHs measured. Error bars indicate one standard deviation. The statistics covers 188 data points for each RH, each corresponding to a 30-min sampling interval.

The transition between the two hygroscopic regimes occurs between 80 and 150 nm, and can have a very individual shape depending on each particular air parcel (Fig. 6). A sharp transition in DHGF necessarily indicates a corresponding transition in chemical particle composition. It is known that cloud processing adds major amounts of soluble material to particles (Hoppel *et al*. 1994). Our HDMPS/TDMPS method can thus help pinpoint the size threshold where soluble particle material as a result of cloud processing becomes increasingly important.

Overall statistics and comparison with earlier observations

As expected, the lowest DHGFs occurred at 30% RH (Fig. 8). The trend of increasing DHGF with increasing particle size, such as observed during the case studies above, could be confirmed for the summary of FIGARO (*see* Table 2). Growth factors derived from the Nano-HDMPS for the particle diameters 10, 30 and 50 nm were added to Table 2. The latter agree with the HDMPS/TDMPS values at 50 nm within the measurement accuracy. From a critical comparison of DHGFs derived from HDMPS/TDMPS as well as the wet and dry Nano-HDMPS, we conclude that the continuous DHGF can be considered valid down to D_p = 70 nm. Below that threshold, the values of DHGF tend to be more variable as a result of a reduced accuracy of the summation method, which assumes a complete conservation of particle number concentration.

We quantitatively compared our DHGFs with hygroscopic growth factors from earlier studies. Hämeri *et al*. (2001) analysed the hygroscopic properties of atmospheric aerosols at SMEAR II in spring and summer 1998–1999 by HTDMA, and we aggregated growth factors (at 90% RH) from their Table 1 as follows: 1.253 at 50 nm, 1.276 at 73 nm, 1.304 at 109 nm, 1.383 at 166 nm, 1.463 at 264 nm. These values compare very well with our DHGFs for particles > 100

nm. Below 100 nm, however, the majority of the data by Hämeri *et al*. (2001) tends to shows bigger growth factors (1.2–1.3) than our results (1.1–1.3, but with the majority of the data lying within 1.1 and 1.2). The comparison with the values by Hämeri *et al*. (2001) is hampered by the fact that they report only data on "periods of externally mixed aerosol" and that the observed aerosols might in fact be very different.

Ehn *et al*. (2007) reported on HTDMA measurements at SMEAR II (at 88% RH) in 2005. Their study concentrates on particle diameters between 20 and 50 nm, so a comparison can be made for that range only. An average growth factor around 1.28 for 50 nm, and 1.20 for 20 nm can be estimated from Ehn *et al*. (2007: fig. 3). These values are largely in line with the observations by Hämeri *et al*. (2001) who used a similar HTDMA, and thus bigger than the average DHGFs determined from our HDMPS/TDMPS and Nano-HDMPS. The reasons why the HTDMA values could be systematically lower than the DHGF values from our study are not clear. The currently available comparisons experiments between HDMPS/TDMPS data processed by the summation method on the one hand, and HTMDA measurements on the other hand, are not sufficient to clarify whether the observed discrepancy in DHGFs below 70 nm is a result of the differing methods, or the different aerosols measured.

Backtrajectory cluster analysis

Cluster method

Back trajectories are a valuable tool to investigate the origin of air pollutants. Consequently, a back trajectory cluster analysis was applied to confirm the source regions of particle number size distributions as well as the variability of DHGF with these different air masses. We applied a *k*-means cluster algorithm (Engler *et al*. 2007), which follows the approach reported originally by Dorling *et al*. (1992). In *k*-means cluster analysis the entire dataset is divided into a predetermined number of trajectory clusters. The resulting clusters should be as distinct as possible from each other but as homogeneous as possible internally. In practice, back trajectories were calculated using the HYSPLIT4 model (HYbrid Single-Particle Lagrangian Integrated Trajectory; Draxler and Hess 2004). A total of 101 back trajectories were computed for every 12 hours (00:00 and 12:00 UTC) of the duration of FIGARO, and are taken as representative of the local time windows of 20:00–08:00 (night) and 08:00–20:00 (day), respectively. The duration of every back trajectory was 96 hours. In addition, vertical profiles of pseudo-potential temperature calculated from the nearest regular radiosonde ascents at Jokioinen, about 130 km southwest of Hyytiälä, were used. For the cluster analysis the trajectory vectors were combined with vertical profiles of the pseudo-potential

Table 2. Mean values and standard deviation of the descriptive hygroscopic growth factor of aerosol particles during FIGARO. Dry reference values determined by the Nano-HDMPS refer to RH < 5%.

D_p (nm)	Instrument	RH = 30%		RH = 55%		RH = 76%		RH = 90%	
		μ	σ	μ	σ	μ	σ	μ	σ
300	HDMPS/TDMPS	1.057	0.028	1.139	0.041	1.261	0.060	1.441	0.094
200	HDMPS/TDMPS	1.058	1.058	1.127	0.044	1.244	0.068	1.409	0.107
150	HDMPS/TDMPS	1.047	0.032	1.109	0.049	1.208	0.069	1.352	0.116
100	HDMPS/TDMPS	1.011	0.022	1.062	0.053	1.132	0.087	1.244	0.122
70	HDMPS/TDMPS	0.980	0.049	1.032	0.061	1.095	0.074	1.193	0.099
50	HDMPS/TDMPS	0.940	0.105	1.000	0.104	1.063	0.101	1.161	0.130
50	Nano-HDMPS	0.999	0.999					1.192	1.192
30	Nano-HDMPS	1.012	0.100					1.178	0.158
10	Nano-HDMPS	1.014	0.154					1.155	0.191

temperature θ_v, such as performed in Engler *et al*. (2007). θ_v was included to reflect the eventual importance of vertical atmospheric stratification for our near-surface measurements. The profiles of θ_v were normalised to the value of zero near the ground so that the profiles are solely a measure of the vertical stability and not the absolute temperature. Distances between back trajectories were calculated in angular degrees according to spherical geometry. Since geographical coordinates (latitude and longitude) and pseudo-potential temperature are merged into a single distance, a suitable weight is required to generate and combine three variables of equitable magnitude. After sequential tests using different weights for the pseudo-potential temperature, a weight of 0.8 K^{-1} was found to separate the size distribution data set most efficiently.

The cluster algorithm was run for a range of cluster numbers between three and eight. Generally, selecting a small number of clusters will generate larger, more representative sub-sets of data. Using a high number of clusters, however, will resolve more features of available aerosol types. We determined a number of seven as a viable compromise between these two aspects. Ten algorithm runs were conducted, each starting with slightly different initial conditions with respect to the orientation of the isotropic seed trajectories. The solution described in the following is the one which decomposed the dry size distribution data set for $D_p > 50$ nm most effectively.

Cluster results

Despite the experiment's relatively short duration, the observations cover a variety of air masses from all directions (*see* Fig. 9).

In particular, the trajectory clusters represent air masses originating from the following regions: North Atlantic (cluster 1), slow air masses from within Scandinavia (2), northwestern Europe (3), the south of European Russia (4), the north of European Russia (5), and the Arctic (6 and 7). Cluster 6 represents easterly air masses passing over the Barents Sea, and cluster 7 represents air masses directly from the polar region. These air masses are associated with different degrees of vertical stability, notably very stable (4), moderately stable (1, 3), less stable (2, 6, 7) and almost neutrally stable. As Fig. 9c shows averages, several cases are included where the atmosphere was neutrally stable or instable within the lowest 2 km.

Broadly speaking, the body of air masses can be divided into two major classes featuring more (4, 3, 5, 2) and less (1, 7, 6) continental influence (Fig. 9d). Not surprisingly, high accumulation mode concentration occurred in the clusters 4 and 5 during the advection of continental air from continental Russia between 6 and 10 May 2004 (DOY 127–131). This observation is consistent with that of Sogacheva *et al*. (2005) who located, on the basis of six years of observations at SMEAR II, the major source areas of accumulation mode particles in eastern Europe and southern Eurasia. It is worth mentioning that continental air masses are generally dry, thereby making the removal of aerosol by precipitation unlikely. Besides, cluster 3, associated with trajectories over the Baltic Sea, showed relatively high accumulation mode concentrations as well. The latter observation might be indicative of ship emissions over the highly trafficked Baltic Sea.

In contrast, the North Atlantic (1) and Artic (6, 7) air masses were characterized by very low accumulation mode concentrations. This is due to the scarcity of anthropogenic sources in the corresponding areas as well as the increased probability of precipitation scavenging with respect to the other clusters. However, the aerosols of clusters 1 and 7 contain a significant Aitken mode with diameter around 40 nm. Aitken particles may originate from biogenic sources over the sea (Raes 1995) or boreal forest (Tunved *et al*. 2006). Recent findings on new particle formation and their growth into the Aitken mode supports that the boreal forest is the dominating source for those particles (Kulmala *et al*. 2004a, Allan *et al*. 2006). Note that this Aitken mode is delineated from the accumulation mode and seems to be largely absent in the clusters of pronounced continental character (3, 4 and 5).

Descriptive hygroscopic growth factors (DHGFs) for RH = 90% are shown in Fig. 9e for each of the seven trajectory clusters. In the accumulation mode range, the mean DHGFs ranged between 1.37 and 1.50, whereas for D_p = 90

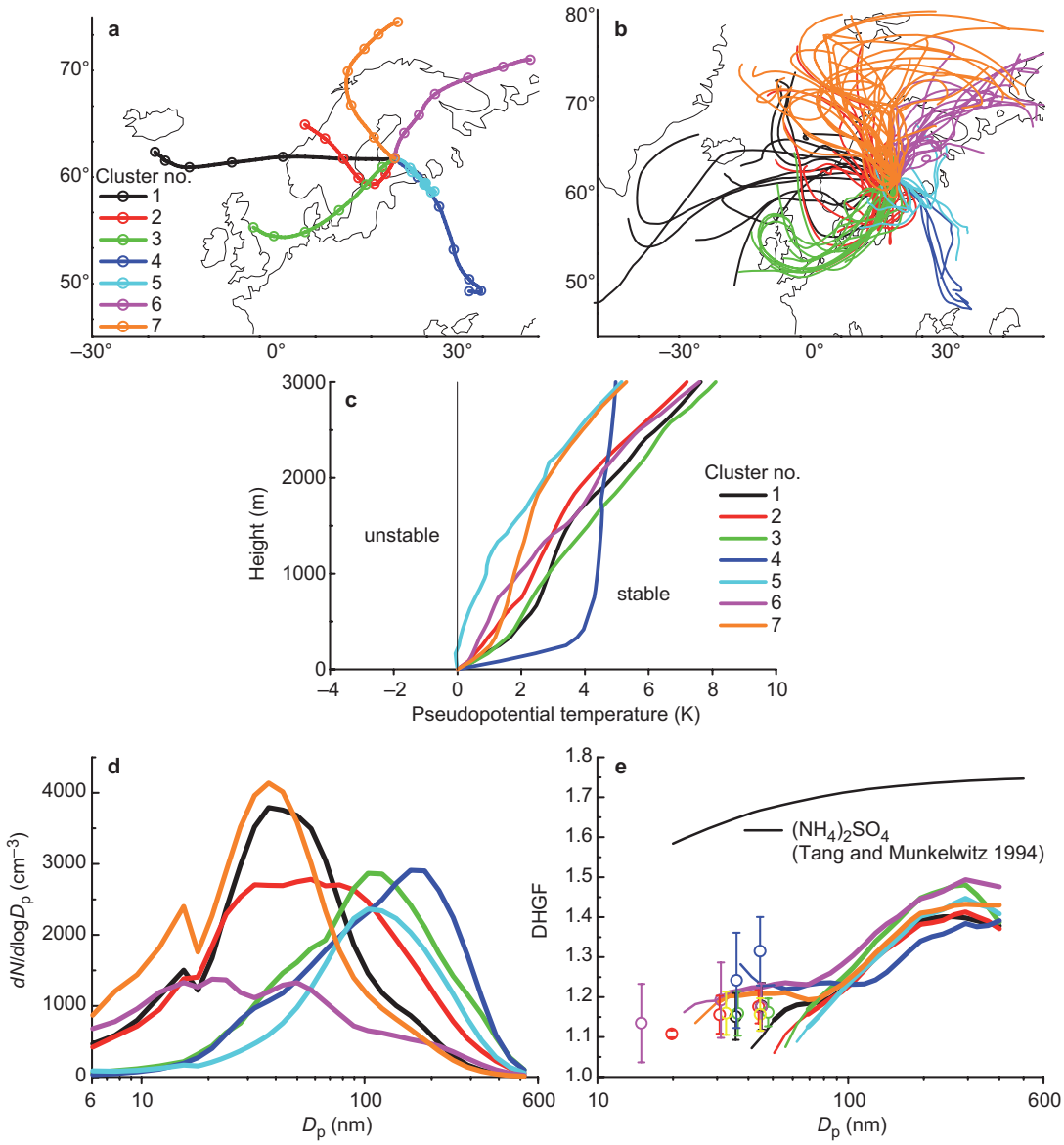

Fig. 9. Results of the back trajectory cluster analysis using seven clusters. (**a**) mean back trajectories, (**b**) individual back 4-day trajectories, (**c**) mean pseudopotential temperature (θ_v) profile above the ground, (**d**) mean particle number size distributions, (**e**) size dependent DHGF at 90% RH. Circles in panel **e** indicate Nano-HDMPS results with whiskers indicating one standard deviation. The growth factor of pure ammonium sulfate particles (Tang and Munkelwitz 1994) was added to illustrate the magnitude of the Kelvin and Raoult effects.

nm, the DHGFs ranged between 1.12 and 1.24. The aerosols in all air masses have in common the above-mentioned increase in DHGF with increasing particle size. Again, we consider this as a result of varying chemical composition, as can be seen from the contrasting growth curve of pure ammonium sulfate particles (Tang and Munkelwitz 1994), which illustrates the magnitude of the Kelvin and Raoult effects.

Below 50 nm, the DHGFs become increasingly uncertain because their calculation is based on the assumption of equal number concentration in the TDMPS and HDMPS. This condition seems not to be met all the time, so that the

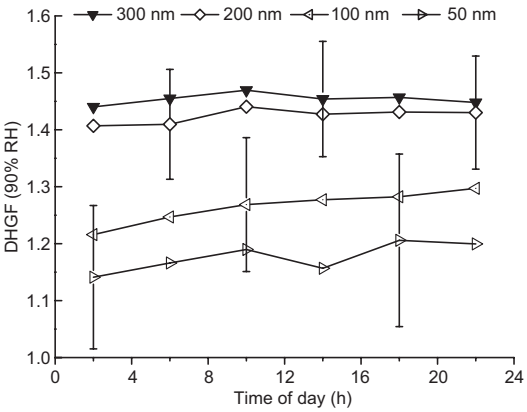

Fig. 10. Diurnal variation of DHGF from TDMPS/HDMPS at 90% RH for several dry particle sizes (D_p = 300, 200, 100, and 50 nm). The data points are plotted in the centre of each 4-hour interval.

DHGF curves eventually diverge at the lowest diameter. To provide more robust numbers below 50 nm, DHGFs obtained from the Nano-HDMPS were added to Fig. 9e. They consolidate the DHGFs of Aitken and nucleation mode particles within a range of mostly 1.1–1.3, and indicate a similar tendency with air masses as the data derived from TDMPS/HDMPS.

There is no obvious correlation between accumulation mode concentration and hygroscopicity (Fig. 9e). The general conclusion is that air mass history only explains a limited part of the observed variation in particle hygroscopicity. It appears that the ambient aerosol at SMEAR II is a relatively constant mixture of soluble as well as insoluble particulate compounds, possibly modulated by cloud processing which could be spatially inhomogeneous and therefore hard to trace experimentally.

Diurnal effects

It is noticeable that little change happens to the DHGF of accumulation mode particles throughout the day (Fig. 10). This result is broadly consistent with the accumulation mode being the long-lived fraction of the atmospheric aerosol. A slight increase, in contrast, by about 0.06 can be noted for the particle sizes 50 and 100 nm. Our trend is consistent with Ehn *et al*. (2007), who reported a diurnal cycle in GF for D_p < 50 nm, which gains in amplitude with decreasing particle size.

Here, we can only speculate about this gradual increase of the growth factor of Aitken particles: Photochemical reactions driven by the hydroxyl radical during day-time may generate low-volatile organic species that condense on the existing particles, and tend to increase the particles' water solubility (cf. Boy *et al*. 2004). The relative mass gain of such soluble species would be the higher the smaller the particles are. Therefore, the addition of soluble material during the course of a day might be evident in the DHGF of particles < 100 nm but not for > 200 nm (*see* Fig. 10). However, this interpretation cannot be considered conclusive without a time-resolved chemical analysis of the particles. Ehn *et al*. (2007) argued that smaller particles (especially < 30 nm) may have a more intensive diurnal cycle because they show the most intense relative gain in soluble mass fraction by highly hygroscopic species, such as sulphuric acid, which condense as a result of daytime photochemical reactions.

Hygroscopic growth and chemical particle composition

The experimentally determined hygroscopic growth factors were compared with values calculated based on chemical composition measurements assuming a simplistic mixture and solubility model. Although the data set available is not ideal, the calculations were carried out in order to cross-check two available data sets.

Chemical composition

Between 7 and 31 May 2004, Saarikoski *et al*. (2005) collected ambient particles at Hyytiälä using a virtual impactor, with the aim to achieve a gravimetric closure for particle mass. A total of ten PM_1 bulk aerosol samples were chemically analysed by these authors for ammonium and sulfate ions, as well as elemental and organic carbon. The study achieved a mass closure for the accumulation mode within 10%, albeit the lack of a relative humidity measurement during

the gravimetric weighing of the impactor samples was expected to reduce the accuracy of the mass closure. Since the sampling periods of Saarikoski *et al*. (2005) coincided with ours, we used their data to initialise a simplistic hygroscopic growth model. We re-iterated the chemical composition of the eight PM_1 bulk aerosol samples of Saarikoski *et al*. (2005) (*see* Table 3) to be employed in the following.

Hygroscopicity model

A simplistic hygroscopic growth model was applied to calculate synthetic growth factors from measured chemical composition. Rather than accounting for the properties of many individual substances in detail, its main intention was to distinguish between highly soluble and insoluble species, respectively. Measurements during FIGARO using a hygroscopic tandem DMA suggested an overwhelmingly mono-modal hygroscopic mixture of sub-μm particles. Thus, our growth model can safely assume a homogeneously mixed aerosol, treating each particle as an insoluble core plus a shell of soluble material. Based on laboratory and field evidence, elemental carbon is considered part of the insoluble class (growth factor 1.0) (Weingartner *et al*. 1997, Massling *et al*. 2005).

For organic carbon, the situation is more diverse, although the contribution of organic carbon to the total water uptake of atmospheric aerosol particles is assumed to be modest compared with the inorganic fraction (McFiggans *et al*. 2005). Atmospheric aerosols dominated by organic matter showed only low growth factors in HTDMA experiments (Petters and Kreidenweis 2007), and a recent closure study between chemical composition and hygroscopic growth of aerosol particles at a coastal site in England yielded an ensemble hygroscopic growth factor of the organic fraction of 1.20 at 90% RH (Gysel *et al*. 2007). Due to the unavailability of information on the composition of organic carbon with respect to individual and/or mass-relevant compounds at the SMEAR-II station, we treated organic carbon as part of the insoluble class of substances as well.

For ammonium sulfate we assume a hygroscopic growth factor based on the water activity parameterisations from Tang and Munkelwitz (1994). Sodium chloride is not included because the source contributions from sea spray have been suggested to be negligible for the particle mass < 500 nm at Hyytiälä (Mäkelä *et al*. 2001, Cavalli *et al*. 2006). These authors also suggested that ammonium sulfate occurs in the form of $(NH_4^+)_2SO_4^{2-}$ rather than $NH_4^+HSO_4^{2-}$ (bisulfate). Table 3 compiles the input data for the hygroscopicity growth model. Based on the concentrations reported, the ion balance between sulfate and ammonium is not matched since NH_4^+ is available in excess as compared with SO_4^{2-} for all samples. Two options to deal with this situation are outlined in the following.

As the first option (model I), we only considered the mass of ammonium and sulfate ions as

Table 3. Mass fractions of several chemical compound classes (after Saarikoski *et al.* 2005) as well as the calculated and measured hygroscopic growth factors. The measured hygroscopic growth factors were averaged between 200 and 300 nm, thus covering the area of the mass mode of the size distribution.

Sampling period	Total mass PM1	Mass fractions (%) (determined at unspecified RH)						Growth factor (200–300 nm)		
	(μg m^{-3})	SO_4^{2-}	NH_4^+	SO_4^{2-} + NH_4^+	OC	EC	REST	Model I	Model II	Measured
7–9 May 2004	16.1	28.3	10.1	38.4	31.4	3.2	26.9	1.381	1.518	1.405
9–11 May 2004	6.3	30.7	10.6	41.4	33.4	2.5	22.7	1.403	1.538	1.526
6–18 May 2004	2.4	31.1	11.2	42.3	30.3	4.1	23.2	1.409	1.557	1.502
18–20 May 2004	1.8	26.4	9.0	35.4	51.7	5.6	7.3	1.358	1.479	1.361
20–22 May 2004	1.5	28.1	10.5	38.6	30.1	5.2	26.1	1.382	1.530	1.521
22–24 May 2004	1.1	29.8	10.5	40.4	35.1	8.8	15.8	1.396	1.533	1.536
24–26 May 2004	2.8	30.7	9.7	40.4	31.8	5.8	22.0	1.396	1.509	1.444
26–28 May 2004	3.4	33.3	9.1	42.5	34.2	4.1	19.2	1.411	1.492	1.432

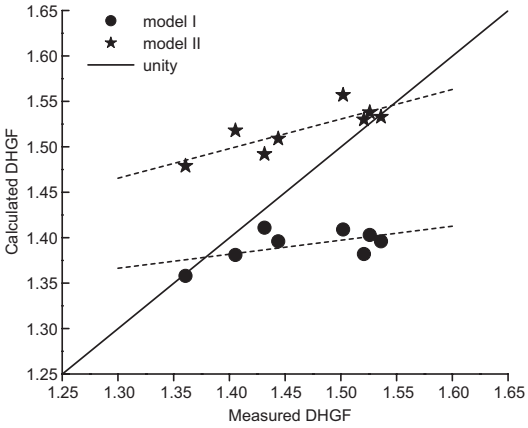

Fig. 11. Comparison between DHGF measured at 250 nm and a modelled hygroscopic particle growth factor based on the eight impactor sampling events listed in Table 3. The particle diameter of 250 nm was chosen for the comparison because it is close to the mass mean diameter of the particles collected with the PM_1 sampler.

the soluble fraction of the particle mass. The sum of these compounds was assumed to grow like an ideal solution of ammonium sulfate, while the rest of the particulate mass was considered to be insoluble.

As the second option (model II), the deficiency in ion balance between ammonium and sulfate ions was calculated first. This deficiency was balanced by a corresponding charge of nitrate ions (NO_3^-). The mass of these nitrate ions was subtracted from the unspecified rest in the mass balance (REST in Table 3). Ammonium sulfate and ammonium nitrate were assumed to grow like an ideal mixed solution (Zdanovskii 1948, Stokes and Robinson, 1966), whereas all other substances, notably OC, EC, and the remainder of the unspecified rest were treated as insoluble.

Results

The calculated growth factors turn out higher for model II because nitrate ions, which are not accounted for in model I, are also considered (Fig. 11 and Table 3). Both models yielded data points that agree with the experimental values but also points that diverge significantly. The lines to the data clouds in Fig. 11 have slopes far from unity, and it appears that the experimental DHGFs show a higher sensitivity to changes in ambient aerosol than those calculated from average bulk chemical composition. Importantly, the differences between modeled and measured DHGFs did not correlate with the OC concentration, which suggests that the ignorance of the hygroscopic growth of organics is not the source of disagreement here. Further conclusions are difficult to justify in view of the uncertainties of the comparison presented here. In the future, it would be desirable to combine hygroscopicity measurements with a more detailed chemical speciation of the particle material, i.e. including the sub-fractions of water soluble and non-soluble organic compounds as well.

Growth factor parameterisation

Based on the measurements conducted between May and July 2004, we developed a robust, universal parameterisation for hygroscopic particle growth in the air masses arriving at SMEAR II. Our parameterisation is based on the median values of 3768 hygroscopic growth factors measured at 30%, 55%, 76% and 90% RH and is considered to represent the average boundary layer aerosol over central Finland in summer. It disregards hygroscopicity modes and describes the average hygroscopicity of all particles at a given dry size. The parameterisation is intended to supplement an earlier expression derived by Laakso *et al*. (2004), whose drawback is that the growth factors calculated for particle diameters outside a specific particle diameter interval become extremely large or negative.

The parameterisation accounts for the functional dependencies of relative humidity (RH; Fig. 12) and dry particle size (D_p; Fig. 8). The latter dependency describes the effects of chemical composition. The dependency of GF as a function of RH was expressed by the hyperbolic function

$$\mathrm{GF}\left(D_\mathrm{p}, \mathrm{RH}\right) = \left(1 - \mathrm{RH}\right)^{-\alpha\left(D_\mathrm{p}\right)}, \qquad (1)$$

with RH given across the range 0–1, and the fit parameter $\alpha(D_p)$ accounting for the observed effects of particle size. The hyperbola used to reproduce the RH dependency was selected from

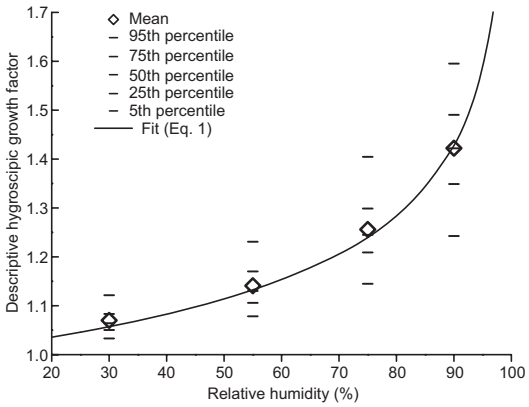

Fig. 12. The descriptive (average) hygroscopic growth factor of dry 200 nm particles as a function of RH.

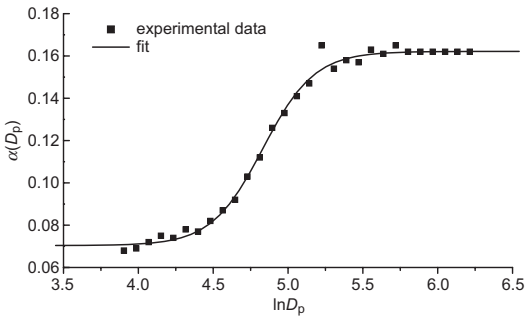

Fig. 13. Variation of the exponent $\alpha(D_p)$ with the natural logarithm of particle diameter. The sigmoidal fit is represented by Eq. 2.

an overview of analytical functions describing atmospheric particle growth (Zhou 2001), and was the function that represented best our experimental data.

In a first step, fits similar to those shown in Fig. 12 were performed for each dry particle size, yielding the experimental function $\alpha(D_p)$. This function was fitted with a sigmoidal function as a function of dry particle diameter D_p:

$$\alpha\left(D_p\right) = 0.16215 - \frac{0.09177}{1+e^{\frac{\ln D_p - 4.83217}{0.17168}}}, \qquad (2)$$

The quality of the fit is illustrated in Fig. 13. Combining Eqs. 1 and 2 provides the parameterisation of GF as a function of RH and D_p. An advantage of Eq. 2 is that it can safely be applied for all particle sizes, although the fit is only supported by data points between 60 and 350 nm. Outside this range the growth factor assumes the asymptotic values of the sigmoidal function. This parameterisation was compared with a previous parameterisation (Laakso *et al*. 2004) based on the HTDMA data determined at Hyytiälä in 2001 (Hämeri *et al*. 2001). For 200 nm and 90%, a difference in GF of 0.023 was found, i.e. small in view of the general uncertainties involved in deriving both parameterisations.

Simulating vertical profiles of CS under changing relative humidity

The formation of new particles (D_p < 30 nm) can be observed frequently at Hyytiälä (Dal Maso *et al*. 2005) and elsewhere in the continental boundary layer (Weber *et al*. 1997, Birmili *et al*. 2003, Kulmala *et al*. 2004b). Although no universal conclusions have been made with respect to the chemical species initiating nucleation, it can safely be assumed that sulfuric acid participates either in the nucleation or the activation process (Kulmala *et al*. 2006). There are several arguments that the probability of nucleation may increase inside a well-mixed boundary layer with height and achieve a maximum near the top of the layer because of diminishing temperature and increasing relative humidity (Weber *et al*. 1999, Nilsson *et al*. 2001, Hellmuth 2006) and/or turbulent mixing in the entrainment zone (Nilsson and Kulmala 1998). A counter-acting effect is the growth of pre-existing particles and the associated condensation sink CS (Kulmala *et al*. 2001) along with increasing RH. If CS increases, condensable precursor gases will condense at larger rates onto pre-existing particles and hence decrease their steady-state concentration, possibly below a level that is critical for the nucleation of new particles.

Due to the absence of radiosounding ascents at Hyytiälä, we used corresponding data (θ_v, water vapour mixing ratio, and RH) from Jokioinen, distant about 300 km. Two days (20 and 25 May 2004) with new particle formation were examined (*see* Fig. 14 for size distribution evolution). The dry size distributions recorded between 10:00 and 14:00 (local time) on each day were used to drive the calculation. The condensation sink CS, i.e. the rate of vapour condensation onto the pre-existing particle population was calcu-

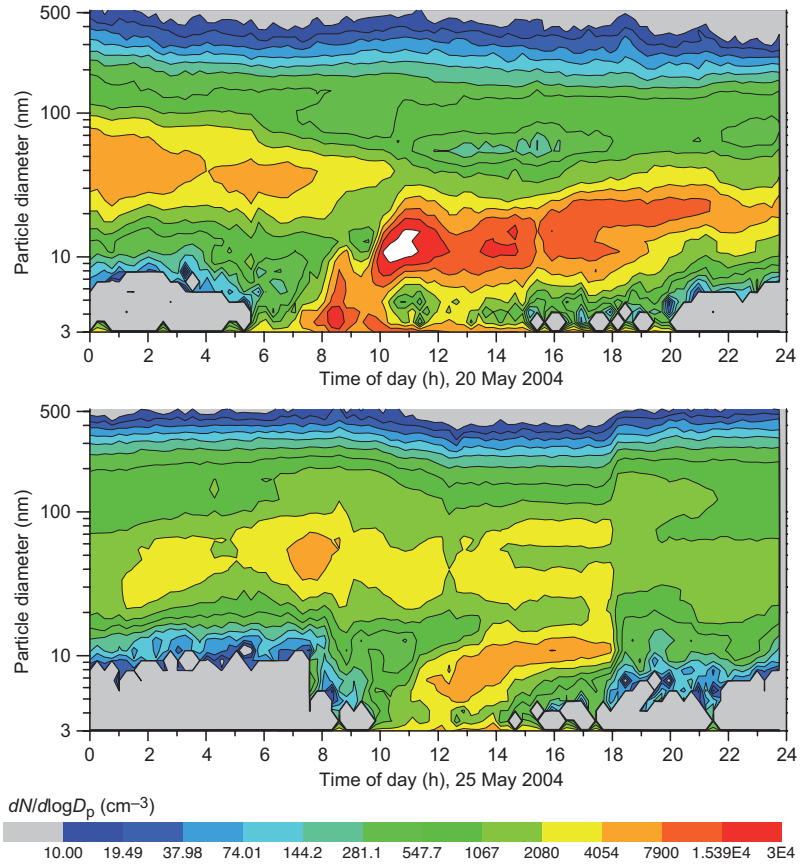

Fig. 14. Dry particle number size distributions on 20 and 25 May 2004, recorded by the TDMPS instrument at SMEAR II. The secondary formation of new particles can be seen by high number concentrations of particles < 30 nm.

lated using the Fuchs-Sutugin form of vapour mass transfer onto particles, assuming molecular sulphuric acid as a condensing species with an accommodation of unity.

A necessary assumption for our simulation is that the dry particle size distribution stays constant within the well-mixed boundary layer. This assumption appears reasonable for Hyytiälä in view of the relatively flat terrain. Hot-air balloon measurements reported such cases of a homogeneous vertical distribution of total particle concentration in the mixed layer (Laakso *et al*. 2007).

In conditions recorded on 20 and 25 May 2004 the values of CS peak near the top of the boundary layer (TBL) (Fig. 15). Consequently, lower concentrations of gas-phase precursors, such as sulphuric acid may be expected near the TBL even in the absence of clouds. Since temperatures are lower near the TBL, however, the saturation ratio is likely to increase as a function of height as well. Based on the RH profiles examined, CS may easily vary by a factor of two within a cloud-free boundary layer. It appears, therefore, advisable that the reported hygroscopic particle growth effects be accounted for in an analysis of boundary layer nucleation. The presented data set on DHGF may contribute to validate the hygroscopic growth modules of more complex boundary layer simulations using multicomponent aerosol dynamics (e.g., Boy *et al*. 2006).

Conclusions

In a joint effort, dry-state and humidified number size distributions of atmospheric particles were characterised in the boreal forest environment with multiple instruments. Such data on humidified size distributions are instrumental in evaluating their optical and aerosol dynamic effects under real atmospheric conditions.

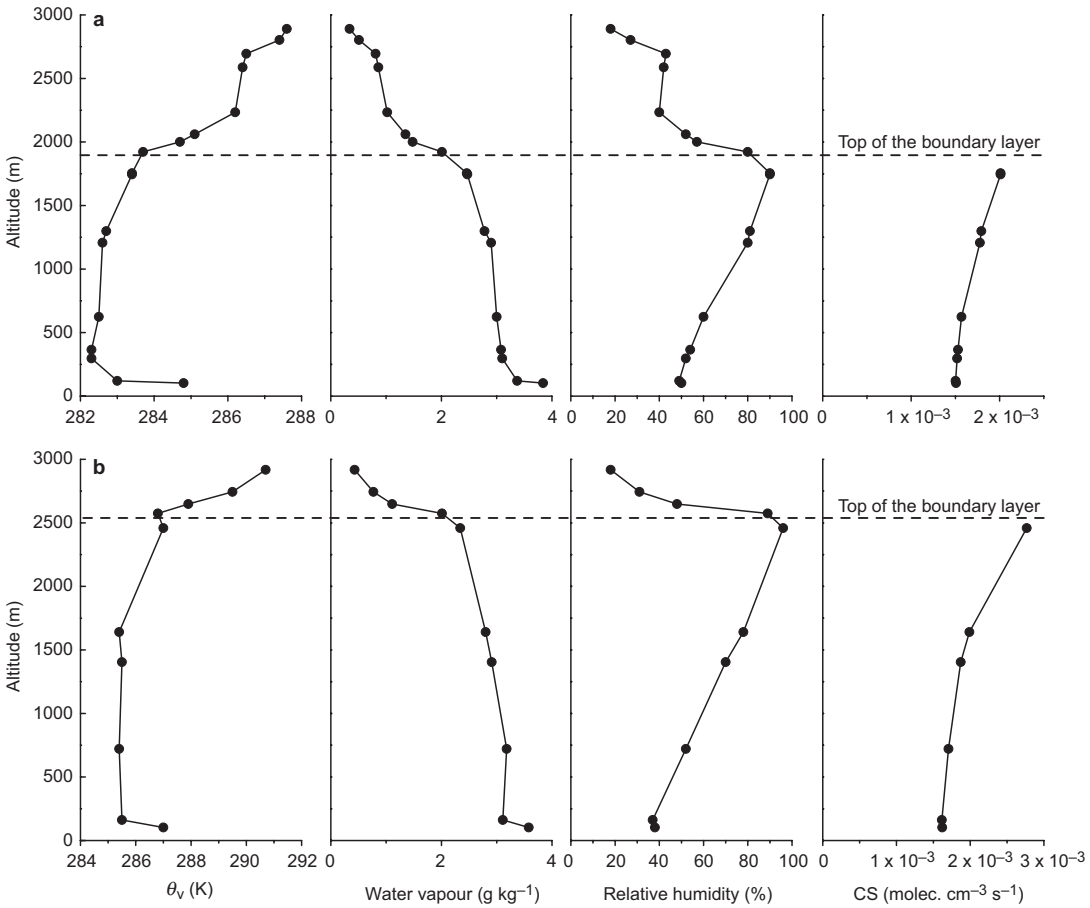

Fig. 15. Vertical profiles of pseudopotential temperature θ_v, water vapour content, relative humidity, and condensation sink rate CS on (**a**) 20 May 2004 and (**b**) 25 May 2004. θ_v, water vapour and RH were taken from radiosounding measurements at Jokioinen, CS was simulated on the basis of the TDMPS measurements near the ground.

The operation of a HDMPS in cycles allows the determination of size distributions (diameter range 20–800 nm) at various controlled relative humidities between 30% and 90%. A combination with concurrent dry TDMPS measurements, and the application of a summation method on the combined data set yielded a descriptive hygroscopic growth factor (DHGF), which averages the hygroscopic growth of all particles at a given dry size.

The results suggested that in air arriving at the SMEAR II station, the hygroscopic growth of ambient particles depended, above all, on particle size. While the hygroscopic growth factors of accumulation mode particles were on average between 1.25 and 1.45 at 90% relative humidity, Aitken and nucleation mode particles were less hygroscopic, and had corresponding growth factors in the ranges 1.20–1.25 and 1.15–1.20, respectively.

The hygroscopic transition between the Aitken and the accumulation modes could be pinpointed to the size interval between 80 and 150 nm, and coincided in many cases with transition between the physical particle modes. Our impression is that the HDMPS/TDMPS technique is able to directly visualise the impact of liquid-phase chemical processes generating soluble material during a previous activation in clouds (Hoppel *et al*. 1994).

While the DHGFs were considered to be most accurate at the upper limit of the range evaluated (diameter 300 nm), their values below 70 nm were considered more uncertain due to

the propagation of accidental errors in the particle size distributions into the calculation of DHGF. It is imperative for the improvement of the HDMPS/TDMPS summation method more sophisticated calibrations and characterisations of the instruments be conducted at the various relative humidities. Nevertheless, DHGFs derived from the Nano-HDMPS instrument could be used to consolidate the atmospheric growth factors of particles smaller than 50 nm at 90% RH to the range 1.1–1.3.

The overall variation of the growth factors with time, however, could only be imperfectly linked to factors such as back trajectories, air masses, or time of day. Based on the body of measurements, an empirical parameterisation for the hygroscopic growth of atmospheric Aitken and accumulation mode particles at Hyytiälä was developed, which may be advantageous for the modelling of wet size distributions or the validation of atmospheric multi-component aerosol models. This parameterisation is assumed to be representative of the atmosphere over the boreal forest under summertime conditions.

Finally, tests were carried out to examine the possible variation of the condensational sink parameter within a well-mixed boundary layer. The calculations suggested that CS may easily vary by a factor of two as a function of altitude, which has consequences on the vertical distribution of the steady-state concentrations of nucleating vapours.

Acknowledgements: We acknowledge Dr. (Hc.) Toivo Pohja for his logistic and technical support, and Nicole Kaaden (IfT) for intermediate data processing. The work was supported by the German Academic Exchange Service (DAAD) under the programme PPP-Finnland 2004, and the Academy of Finland (project nos. 211483, 211484, 1118615, 110763 and 113804). We finally thank the two anonymous reviewers who helped to improve and enhance this paper.

References

Allan J.D., Alfarra M.R., Bower K.N., Coe H., Jayne J.T., Worsnop D.R., Aalto P.P., Kulmala M., Hyötyläinen T., Cavalli F. & Laaksonen A. 2006. Size and composition measurements of background aerosol and new particle growth in a Finnish forest during QUEST 2 using an aerodyne aerosol mass spectrometer. *Atmos. Chem. Phys.* 6: 315–327.

Birmili W., Stratmann F. & Wiedensohler A. 1999. Design of a DMA-based size spectrometer for a large particle size range and stable operation. *J. Aerosol Sci.* 30: 549–553.

Birmili W., Berresheim H., Plass-Dülmer C., Elste T., Gilge S., Wiedensohler A. & Uhrner U. 2003. The Hohenpeissenberg aerosol formation experiment (HAFEX): a long-term study including size-resolved aerosol, H_2SO_4, OH, and monoterpenes measurements. *Atmos. Chem. Phys.* 3: 361–376.

Birmili W., Nowak A., Schwirn K., Lehmann K., Massling A. & Wiedensohler A. 2004. A new method to accurately relate dry and humidified number size distributions of atmospheric aerosols. *J. Aerosol Sci.* 35: S15–S16.

Boy M., Petäjä T., Dal Maso M., Rannik Ü., Rinne J., Aalto P., Laaksonen A., Vaattovaara P., Joutsensaari J., Hoffmann T., Warnke J., Apostolaki M., Stephanou E.G., Tsapakis M., Kouvarakis A., Pio C., Carvalho A., Römpp A., Moortgat G., Spirig C., Guenther A., Greenberg J., Ciccioli P. & Kulmala M. 2004. Overview of the field measurement campaign in Hyytiälä, August 2001 in the framework of the EU project OSOA. *Atmos. Chem. Phys.* 4: 657–678.

Boy M., Hellmuth O., Korhonen H., Nilsson E.D., ReVelle D., Turnipseed A., Arnold F. & Kulmala M. 2006. MALTE: model to predict new aerosol formation in the lower troposphere. *Atmos. Chem. Phys.* 6: 4499–4517.

Brechtel F. & Kreidenweis S. 2000. Predicting particle critical supersaturation from hygroscopic growth measurements in the humidified TDMA, part I: Theory and sensitivity studies. *J. Atmos. Sci.* 57: 1854–1871.

Cavalli F., Facchini M.C., Decesari S., Emblico L., Mircea M., Jensen N.R. & Fuzzi S. 2006. Size-segregated aerosol chemical composition at a boreal site in southern Finland, during the QUEST project. *Atmos. Chem. Phys.* 6: 993–1002.

Dal Maso M., Kulmala M., Riipinen I., Wagner R., Hussein T., Aalto P.P. & Lehtinen K.E.J. 2005. Formation and growth of fresh atmospheric aerosols: eight years of aerosol size distribution data from SMEAR II, Hyytiälä, Finland. *Boreal Env. Res.* 10: 323–336.

Dorling S.R., Davies T.D. & Pierce C.E. 1992. Cluster analysis: a technique for estimating the synoptic meteorological controls on air and precipitation chemistry method and applications. *Atmos. Env.* 26A: 2575–2581.

Draxler R. & Hess G. 2004. *Description of the HYSPLIT4 modeling system*. NOAA Technical Memorandum, ERL, ARL-224.

Ehn M., Petäjä T., Aufmhoff H., Aalto P., Hämeri K., Arnold F., Laaksonen A. & Kulmala M. 2007. Hygroscopic properties of ultrafine aerosol particles in the boreal forest: diurnal variation, solubility and the influence of sulfuric acid. *Atmos. Chem. Phys.* 7: 211–222.

Eichel C., Krämer M., Schütz L. & Wurzler S. 1996. The water-soluble fraction of atmospheric aerosol particles and its influence on the cloud microphysics. *J. Geophys. Res.* 101: 29499–29510.

Engler C., Rose D., Wehner B., Wiedensohler A., Brüggemann E., Gnauk T., Spindel G., Tuch T. & Birmili W. 2007. Size distributions of non-volatile particle residuals (D_p < 800 nm) at a rural site in Germany and relation to

air mass origin. *Atmos. Chem. Phys.* 7: 5785–5802.

Gassó S., Hegg D.A., Covert D.S., Collins D., Noone K.J., Ostrom E., Schmid B., Russell P.B., Livingstone J.M., Durkee P.A. & Jonsson H. 2000. Influence of humidity on the aerosol scattering coefficient and its effect on the upwelling radiance during ACE2. *Tellus* 52B: 546–567.

Gysel M., Weingartner E., Nyeki S., Paulsen D., Baltensperger U., Galambos I. & Kiss G. 2004. Hygroscopic properties of watersoluble matter and humic-like organics in atmospheric fine aerosol. *Atmos. Chem. Phys.* 4: 35–50.

Gysel M., Crosier J., Topping D.O., Whitehead J.D., Bower K.N., Cubison M.J., Williams P.I., Flynn M.J., McFiggans G.B. & Coe H. 2007. Closure study between chemical composition and hygroscopic growth of aerosol particles during TORCH2. *Atmos. Chem. Phys.* 7: 6131–6144.

Hämeri K., Väkevä M., Hansson H.-C. & Laaksonen A. 2000. Hygroscopic growth of ultrafine ammonium sulphate aerosol measured using an ultrafine tandem differential mobility analyzer, *J. Geophys. Res.* 105: 22231–22242.

Hämeri K., Väkevä M., Aalto P., Kulmala M., Swietlicki E., Jingchuan Z., Winfried S., Becker E. & O'Dowd C.D. 2001. Hygroscopic and CCN properties of aerosol particles in boreal forests. *Tellu*s 53B: 359–379.

Hänel G. 1976. The properties of atmospheric aerosol particles as functions of the relative humidity at thermodynamic equilibrium with the surrounding moist air. *Adv. Geophys.* 19: 74–188.

Hänel G. & Lehmann M. 1981. Equilibrium size of aerosol particles and relative humidity: new experimental data from various aerosol types and their treatment for cloud physics application. *Contrib. Atmos. Phys.* 54: 57–71.

Hari P. & Kulmala M. 2005. Station for Measuring Ecosystem–Atmosphere Relations (SMEAR II). *Boreal Env. Res.* 10: 315–322.

Hennig T., Massling A., Brechtel F. & Wiedensohler A. 2005. A tandem DMA for highly temperature-stabilized hygroscopic particle growth measurements between 90% and 98% relative humidity. *J. Aerosol Sci.* 36: 1210–1223.

Hellmuth O. 2006. Columnar modelling of nucleation burst evolution in the convective boundary layer: first results from a feasibility study, part III: Preliminary results on physicochemical model performance using two "clean air mass" reference scenarios. *Atmos. Chem. Phys.* 6: 4231–4251.

Hoppel W., Frick G., Fitzgerald J. & Larson R. 1994. Marine boundary layer measurements of new particle formation and the effects nonprecipitating clouds have on aerosol size distribution. *J. Geophys. Res.* 99: 14443–14459.

Im J.-S., Saxena V. & Wenny B. 2001. An assessment of hygroscopic growth factors for aerosols in the surface boundary layer for computing direct radiative forcing. *J. Geophys. Res.* 106: 20213–20224.

Joutsensaari J., Vaattovaara P., Vesterinen M., Hämeri K. & Laaksonen A. 2001. A novel tandem differential mobility analyzer with organic vapor treatment of aerosol particles. *Atmos. Chem. Phys.* 1: 51–60.

Khvorostyanov V. & Curry J. 1999. A simple analytical model of aerosol properties with account for hygroscopic growth: 1. Equilibrium size spectra and cloud condensation nuclei activity spectra. *J. Geophys. Res.* 104: 2175–2184.

Kinne S., Lohmann U., Feichter J., Schulz M., Timmreck C., Ghan S., Easter R., Chin M., Ginoux P., Takemura T., Tegen I., Koch D., Herzog M., Penner J., Pitari G., Holben B., Eck T., Smirnov A., Dubovik O., Slutsker I., Tanre D., Torres O., Mishchenko M., Geogdzhayev I., Chu D.A. & Kaufman Y. 2003. Monthly averages of aerosol properties: A global comparison among models, satellite data, and AERONET ground data. *J. Geophys. Res.* 108(D20), 4634, doi:10.1029/2001JD001253.

Kulmala M., Dal Maso M., Mäkelä J.M., Pirjola L., Väkevä M., Aalto P., Miikkulainen P., Hämeri K. & O'Dowd C. 2001. On the formation, growth and composition of nucleation mode particles. *Tellus* 53B: 479–490.

Kulmala M., Suni T., Lehtinen K.E.J., Dal Maso M., Boy M., Reissel A., Rannik Ü., Aalto P., Keronen P., Hakola H., Bäck J., Hoffmann T., Vesala T. & Hari P. 2004a. A new feedback mechanism linking forests, aerosols, and climate. *Atmos. Chem. Phys.* 4: 557–562.

Kulmala M., Vehkamäki H., Petäjä T., Dal Maso M., Lauri A., Kerminen V.-M., Birmili W. & McMurry P.H. 2004b. Formation and growth rates of ultrafine atmospheric particles: a review of observations. *J. Aerosol Sci.* 35: 143–176.

Kulmala M., Lehtinen K.E.J. & Laaksonen A. 2006. Cluster activation theory as an explanation of the linear dependence between formation rate of 3 nm particles and sulphuric acid concentration. *Atmos. Chem. Phys.* 6: 787–793.

Laakso L., Grönholm T., Kulmala L., Haapanala S., Hirsikko A., Lovejoy E.R., Kazil J., Kurtén T., Boy M., Nilsson E.D., Sogachev A., Riipinen I., Stratmann F. & Kulmala M. 2007. Hot-air balloon as a platform for boundary layer profile measurements during particle formation. *Boreal Env. Res.* 12: 279–294.

Laakso L., Petäjä T., Lehtinen K.E.J., Kulmala M., Paatero J., Hõrrak U., Tammet H. & Joutsensaari J. 2004. Ion production rate in a boreal forest based on ion, particle and radiation measurements. *Atmos. Chem. Phys.* 4: 1933–1943.

Mäkelä J.M., Yli-Koivisto S., Hiltunen V., Seidl W., Swietlicki E., Teinilä K., Sillanpää M., Koponen I.K., Paatero J., Rosman K. & Hämeri K. 2001. Chemical composition of aerosol during particle formation events in boreal forest. *Tellus* 53B: 380–393.

Massling A., Stock M. & Wiedensohler A. 2005. Diurnal, weekly, and seasonal variation of hygroscopic properties of submicrometer urban aerosol particles. *Atmos. Environ.* 39: 3911–3922.

McFiggans G., Alfarra M.R., Allan J., Bower K., Coe H., Cubison M., Topping D., Williams P., Decesari S., Facchini C. & Fuzzi S. 2005. Simplification of the representation of the organic component of atmospheric particulates. *Faraday Discuss.* 130: 341–362.

Nessler R., Bukowiecki N., Henning S., Weingartner E., Calpini B. & Baltensperger U. 2003. Simultaneous dry and ambient measurements of aerosol size distributions at the Jungfraujoch. *Tellus* 55B: 808–819.

Nilsson E.D. & Kulmala M. 1998. The potential for atmos-

pheric mixing processes to enhance the binary nucleation rate. *J. Geophys. Res.* 103: 1381–1389.

Nilsson E.D., Rannik Ü., Kulmala M., Buzorius G. & O'Dowd C.D. 2001. Effects of continental boundary layer evolution, convection, turbulence, and entrainment on aerosol formation. *Tellus* 53B: 441–461.

Nowak A. 2006. *Das feuchte Partikelgrößenspektrometer: Eine neue Messmethode zur Bestimmung von Partikelgrößenverteilungen (< 1 µm) und größenaufgelösten hygroskopischen Wachstumsfaktoren bei definierten Luftfeuchten*. Ph.D. thesis, University of Leipzig, Germany.

Ogren J. & Charlson R. 1992. Implications for models and measurements of chemical inhomogeneities among cloud droplets. *Tellus* 44B: 489–504.

Orr C., Hurd F. & Corbett W. 1958. Aerosol size and relative humidity. *J. Colloid Sci.* 13: 472–482.

Petäjä T., Kerminen V.-M., Hämeri K., Vaattovaara P., Joutsensaari J., Junkermann W., Laaksonen A. & Kulmala M. 2005. Effects of SO_2 oxidation on ambient aerosol growth in water and ethanol vapours. *Atmos. Chem. Phys.* 5: 767–779.

Petters M.D. & Kreidenweis S.M. 2007. A single parameter representation of hygroscopic growth and cloud condensation nucleus activity. *Atmos. Chem. Phys.* 7: 1961–1971.

Rader D. & McMurry P. 1986. Application of the tandem differential mobility analyzer to studies of droplet growth or evaporation. *J. Aerosol Sci.* 17: 771–787.

Raes F. 1995. Entrainment of free tropospheric aerosols as a regulating mechanism for cloud condensation nuclei in the remote boundary layer. *J. Geophys. Res.* 100: 2893–2903.

Rissler J., Vestin A., Swietlicki E., Fisch G., Zhou J., Artaxo P. & Andreae M.O. 2006. Size distribution and hygroscopic properties of aerosol from dry-season biomass burning in Amazonia. *Atmos. Chem. Phys.* 6: 471–491.

Stokes R.H. & Robinson R.A. 1966. Interactions in aqueous nonelectrolyte solutions. I. Solute-solvent equilibria. *J. Phys. Chem.* 70: 2126–2130.

Saarikoski S., Mäkelä T., Hillamo R., Aalto P., Kerminen V.-M. & Kulmala M. 2005. Physico-chemical characterization and mass closure of size-segregated atmospheric aerosols in Hyytiälä, Finland. *Boreal Env. Res.* 10: 385–400.

Saxena P. & Hildemann L. 1996. Water-soluble organics in atmospheric particles: a critical review of the literature and application of thermodynamics to identify candidate compounds. *J. Atmos. Chem.* 24: 57–109.

Seinfeld J.H. & Pandis S.P. 1998. *Atmospheric chemistry and physics* (2nd ed.). John Wiley, New York.

Sogacheva L., Dal Maso M., Kerminen V.-M. & Kulmala M. 2005. Probability of nucleation events and aerosol particle concentration in different air mass types arriving at Hyytiälä, southern Finland, based on back trajectories analysis. *Boreal Env. Res.* 10: 479–491.

Stokes R. & Robinson, R. 1966. Interactions in aqueous nonelectrolyte solutions. i. solute-solvent equilibria. *J. Phys. Chem.* 70: 2126–2131.

Swietlicki E., Hansson H.-C., Hämeri K., Svenningsson B., Massling A. McFiggans G., McMurry P.H., Petäjä T., Tunved P., Gysel M., Topping D., Weingartner E., Baltensperger U., Rissler J., Wiedensohler A. & Kulmala M. 2008. Hygroscopic properties of submicrometer atmospheric aerosol particles measured with H-TDMA instruments in various environments — a review. *Tellus* 60B: 432–469.

Tang I. & Munkelwitz H. 1994. Water activities, densities, and refractive indices of aqueous sulfates and sodium nitrate droplets of atmospheric importance. *J. Geophys. Res.* 99: 18801–18808.

Tang I., Wong W. & Munkelwitz H. 1981. The relative importance of atmospheric sulfates and nitrates in visibility reduction. *Atmos. Environ.* 15: 2463–2471.

Thudium J. 1978. Water uptake and equilibrium sizes of aerosol particles at high relative humidities: Their dependence on the composition of the water-soluble material. *Pure Appl. Geophys.* 116: 130–148.

Tunved P., Hansson H.-C., Kerminen V.-M., Ström J., Dal Masso M., Lihavainen H., Viisanen Y., Aalto P.P., Komppula M. & Kulmala M. 2006. High natural aerosol loading over boreal forests. *Science* 312: 261–263.

Väkevä M., Kulmala M., Stratmann F. & Hämeri K. 2002. Field measurements of hygroscopic properties and state of mixing of nucleation mode particles. *Atmos. Chem. Phys.* 2: 55–66.

Voutilainen A., Kolehmainen V. & Kaipio J.P. 2001. Statistical inversion of aerosol size measurement data. *Inverse Probl. Eng.* 9: 67–94.

Weber R.J., Marti J.J., McMurry P.H., Eisele F.L., Tanner D.J. & Jefferson A. 1997. Measurement of new particle formation and ultrafine particle growth rates at a clean continental site. *J. Geophys. Res.* 102: 4375–4385.

Weber R.J., McMurry P.H., Malaudin R.III, Tanner D., Eisele F., Clarke A. & Kapustin V.N. 1999. New particle formation in the remote troposphere: a comparison of observations at various sites. *Geophys. Res. Lett.* 26: 307–310.

Weingartner E., Burtscher H. & Baltensperger U. 1997. Hygroscopic properties of carbon and Diesel soot particles. *Atmos. Environ.* 31: 2311–2327.

Weingartner E., Gysel M. & Baltensperger U. 2002. Hygroscopicity of aerosol particles at low temperatures — 1. New low-temperature H-TDMA instrument: setup and first applications. *Environ. Sci. Technol.* 36: 55–62.

Winkler P. 1972. The growth of atmospheric aerosol particles as a function of the relative humidity — I. Method and measurements at different locations. *J. Rech. Atmos.* 12: 822–826.

Winklmayr W., Reischl G.P., Linde A.O. & Berner A. 1991. A new electromobility spectrometer for the measurement of aerosol size distributions in the size range from 1 to 1000 nm. *J. Aerosol Sci.* 22: 289–296.

Zdanovskii A. 1948. New methods for calculating solubilities of electrolytes in multicomponent systems. *Zhur. Fiz. Khim* 22: 1475–1485.

Zhou J. 2001. *Hygroscopic properties of atmospheric aerosol particles in various environments*. Ph.D. thesis, University of Lund, Division of Nuclear Physics, Sweden.